ESRF Experimental Report

CH 5695: In-operando SAXS studies of bi-modal Pt/C fuel cell catalysts

Principal Investigator	Professor Matthias Arenz, University of Bern
Co-Proposers	Dr. Jakub Drnec, ESRF
	Professor Mehtap Oezaslan, University of Braunschweig
	Dr Isaac Martens, ESRF
Local contact	Dr. Jakub Drnec

Start of Experiment	09 Sep 2020	**Beamline/#shifts**	ID31/15

1. Abstract

In the work we combined *operando* small- and wide-angle X-ray scattering (SAXS, WAXS) in grazing incidence configuration as a new approach to provide depth-dependent insights into the changes in mean particle sizes and phase fractions occurring for fuel cell catalysts during accelerated stress tests (ASTs). As fuel cell catalyst, a bimodal Pt/C catalyst was chosen that consists of two distinguishable particle size populations. The presence of the two different sizes should favor and uncover electrochemical Ostwald ripening as the major degradation mechanism, i.e., it was expected that the size of the larger particles in the Pt/C catalyst grows at the expense of the smaller particles. The grazing incidence mode revealed an intertwinement of the depth dependent degradation. While the larger particles show the same particle size changes close to the electrolyte-catalyst interface and within the catalyst layer, for the smaller Pt nanoparticles a different degradation scenario is observed. At the electrolyte-catalyst interface, the smaller particles increase in size while their phase fraction decreases during the AST. However, in the inner catalyst layer the phase fraction of smaller particles increases instead of decreases. The results of a depth-dependent degradation strongly suggest the need for a depth-dependent catalyst design for future improvement of the catalyst stability.

2. Experiment details

Due to the COVID restrictions the experiments were performed in remote mode by the Beamline staff, Dr. Drnec, Dr. Martens, and Dr. Chattot. Despite this challenging circumstances, thanks to a good communication, the experiments could be performed mostly as planned. The samples were prepared as catalyst film on a gas diffusion layer (GDL) fitting to the electrochemical cell of the ID31 beamline team[1]. The catalyst was a mixture of two commercial Pt/C catalysts (TEC10E20A and TEC10E50E-HT) achieving bimodal particle distributions. Ar saturated 0.1 M $HClO_4$ was used as electrolyte. Activation of the catalyst was done by 10 cyclic voltammograms (CVs) between 0.06 and 1.0 V versus reversible hydrogen electrode (V_{RHE}) using a scan rate of 50 mV/s. ASTs applying potential steps between 0.6 and 1.0 V_{RHE} (3 s holding per potential) simulating load-cycle conditions in a fuel cell vehicle were performed.

3. Results

Analysis of SAXS / WAXS data: Representative SAXS / WAXS data recorded during the beamtime are shown in Figure 1. Based on the fact that the bimodal Pt/C catalyst is the result of mixing two individually characterized Pt/C catalysts in known metal ratio (0.4:0.6 based on metal weight percentage of the two catalysts), the determined mean particle sizes and phase fractions in the bimodal Pt/C catalysts can be compared to the "expected values". The analysis showed that the mean particle size of both populations of the bimodal catalyst can be determined by SAXS data analysis with high accuracy. However, a quantitative analysis of the relative number of NPs in the two size populations was difficult. The particle diameters and their standard deviations retrieved from the log-normal distributions obtained from the SAXS data are 1.7 ± 0.5 and 5.5 ± 1.5 nm. Comparing the individual catalysts with the prepared bimodal catalyst, it can be demonstrated that the SAXS results are in good agreement with the TEM data of ca. 2 and ca. 5 nm average size. Although the expected relative number of NPs in the two size populations could be fitted to the SAXS data, in simulations the fit is ambiguous in this respect, i.e., no one-to-one correspondence between the intensities of the two populations of the same scattering data is found.
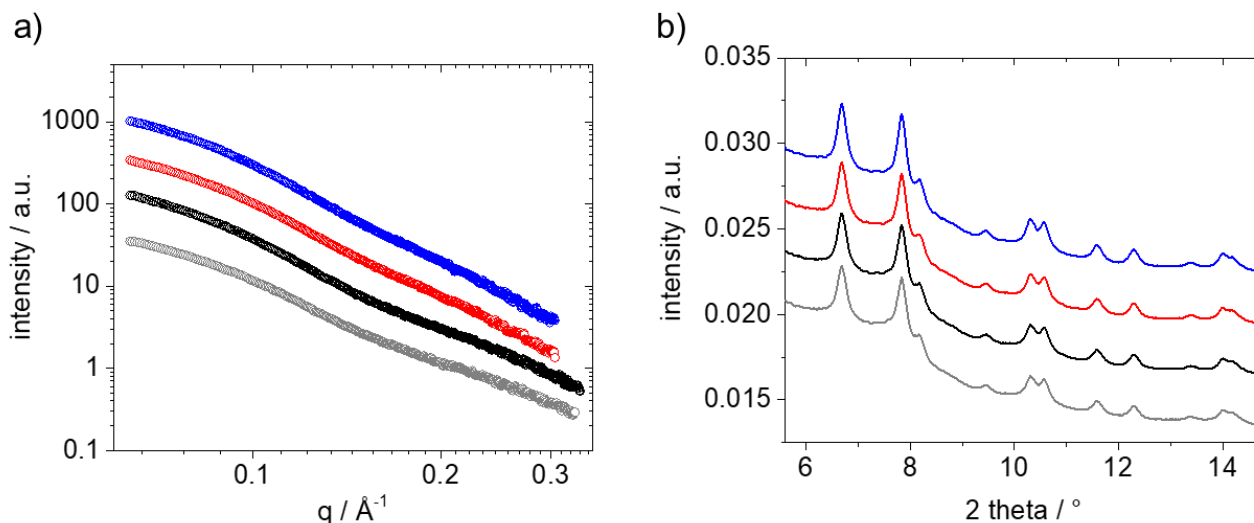
Figure 1. Background subtracted SAXS scattering data and b) WAXS diffractograms in an angular range from 5 to 15 ° 2 theta in the depth close to the electrolyte-catalyst interface: initial (grey), after catalyst cleaning (black), after 2500 AST cycles (red), after 5000 AST cycles (blue). The increase of the height and narrowing of the peaks of the diffractogram during the AST protocol imply an increase in particle size, which is in agreement with the mean particle size results. The data in a) and b) are shown with a vertical offset to improve visibility of the different datasets.

However, this is not the case for the mean particle sizes, which remain the similar in simulations of different phase fractions of the two populations. To address this limitation, we took advantage of WAXS data. The WAXS diffraction patterns clearly show the typical Bragg peaks of the platinum *fcc* phase which are convoluted with the signals of the carbon and polymer background at low 2θ angles. From an angular range of six 2θ onwards, the platinum reflections are virtually free of background and could readily be analyzed by Rietveld refinement.[2] Simultaneously varying both the fraction and crystallite size of the two populations of Pt NPs in the Rietveld refinement of WAXS data was not feasible due to the intertwining of these variables, as only one population with an average coherent domain size was obtained. Therefore, we used the mean particle size of the two populations derived by the SAXS fitting as pre-defined input values in the Rietveld refinement of the WAXS data. Two platinum phases of different coherent domain sizes (input of SAXS mean particle sizes) were used as the structural model in the Rietveld refinement. Although, the mean particle size derived from the SAXS fitting is not identical with the coherent domain size in diffraction, the two parameters are closely related.[1] In this way the fractions of the platinum phases, i.e., their mass ratios, can be determined for the two size populations of Pt NPs. A representative refinement showing the two platinum phases of the structural model with different crystallite sizes is depicted in Figure 2. The obtained ratio of the smaller to the larger population of 0.44:0.56 in the pristine sample close to electrolyte-catalyst interface obtained from the combined SAXS and WAXS data analysis is in good agreement with the theoretical ratio of 0.4:0.6 expected from the sample preparation procedure.
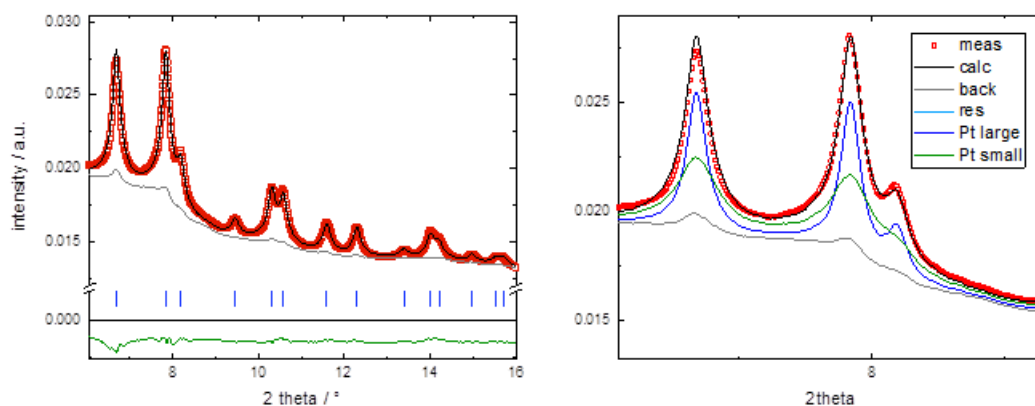

Figure 2. Representative Rietveld refinement of WAXS data based on the structural model including two platinum fcc phases (the blue dashes indicate the position of platinum reflections) of equal lattice parameter (a = 3.9046) with two different coherent domain sizes (2.1 nm and 5.4 nm) in an angular range from six to sixteen two theta (R_{wp} = 0.25 %).

Results: The degradation of the Pt/C catalyst close to the catalyst-electrolyte layer shows features that can be associated with preferential dissolution of small Pt particles and potentially with Ostwald ripening via Pt species mobile on the carbon support, see Figure 3. Starting the AST, the average particle size of the smaller population slightly increases while the phase fraction decreases during the AST. The increase in average size indicates that within the population smaller particles preferentially dissolve and Pt species redeposit on the nanometer scale, the decrease in phase fraction indicates that dissolution is more pronounced in the small population.
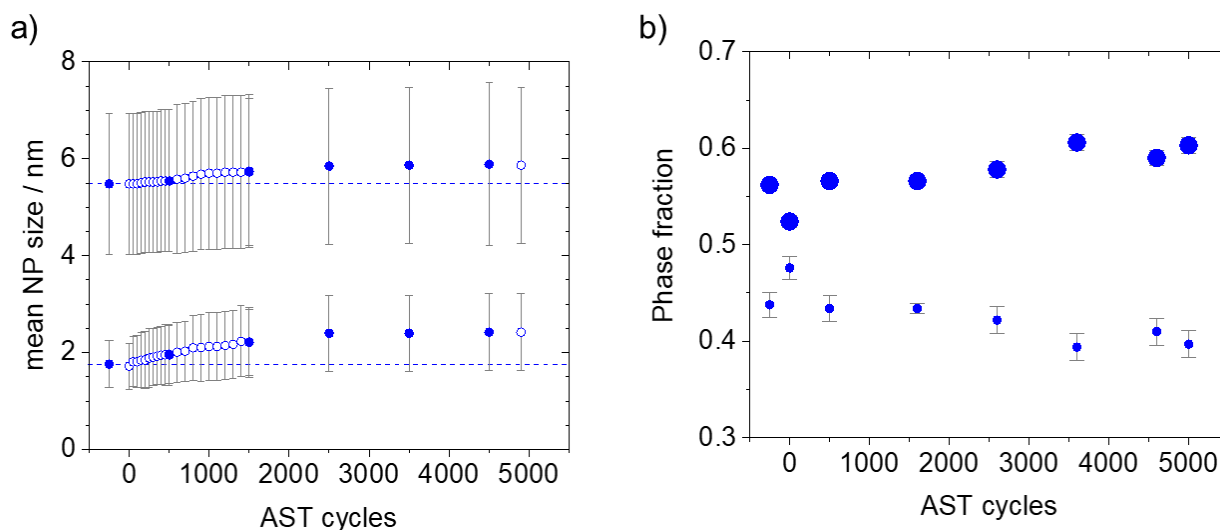

Figure 3. a) Mean particle size of the bimodal Pt NP/C catalyst in the depth close to the electrolyte-catalyst interface plotted together with the standard deviation of a log-normal distribution applying load-cycle conditions as AST protocol in an operando cell after the AST cycles (blue open circles) and after performed CVs (blue filled cycles). b) Phase fractions of the two size populations (small and large circles, for the smaller and larger size populations, respectively) obtained from Rietveld refinement of in the depth close to electrolyte-catalyst interface, keeping the particle sizes determined via SAXS constant. The data points of the pristine sample are given on the x-axis for a negative AST number.

However, in the inner catalyst layer, the phase fraction of the smaller particles increases instead, see Figure 4. Furthermore, the mean particle size of the small population is larger at the inner catalyst layer. By comparison, the mean particle size of the larger population seems homogenous across the catalyst layer and in all cases a slight increase in size is observed during the AST. Although the increase in phase fraction of the smaller particles is difficult to explain at this point, the results show that the degradation of the Pt/C catalyst within the layers is far from being homogeneous. This raises the question if the liquid electrolyte has any influence on the observed mechanism. Interestingly, it is seen that contacting the catalyst with the electrolyte and applying cleaning cycles, the same increase in phase fraction of the smaller particles is observed. It can be speculated that the contact of the electrolyte leads to a pronounced particle loss mechanism, as has previously been observed. In any case, the fact that the observed change in phase fraction is not associated with an increase in mean size suggests that this degradation process is not intrinsically size-dependent but more related to the different catalyst synthesis procedures of both catalysts, in particular - the 'HT' from the commercial name implied - heat treatment (TEC10E50E-HT) of the larger population may lead to a pronounced degradation upon contact to the electrolyte and by applying cleaning cycles.
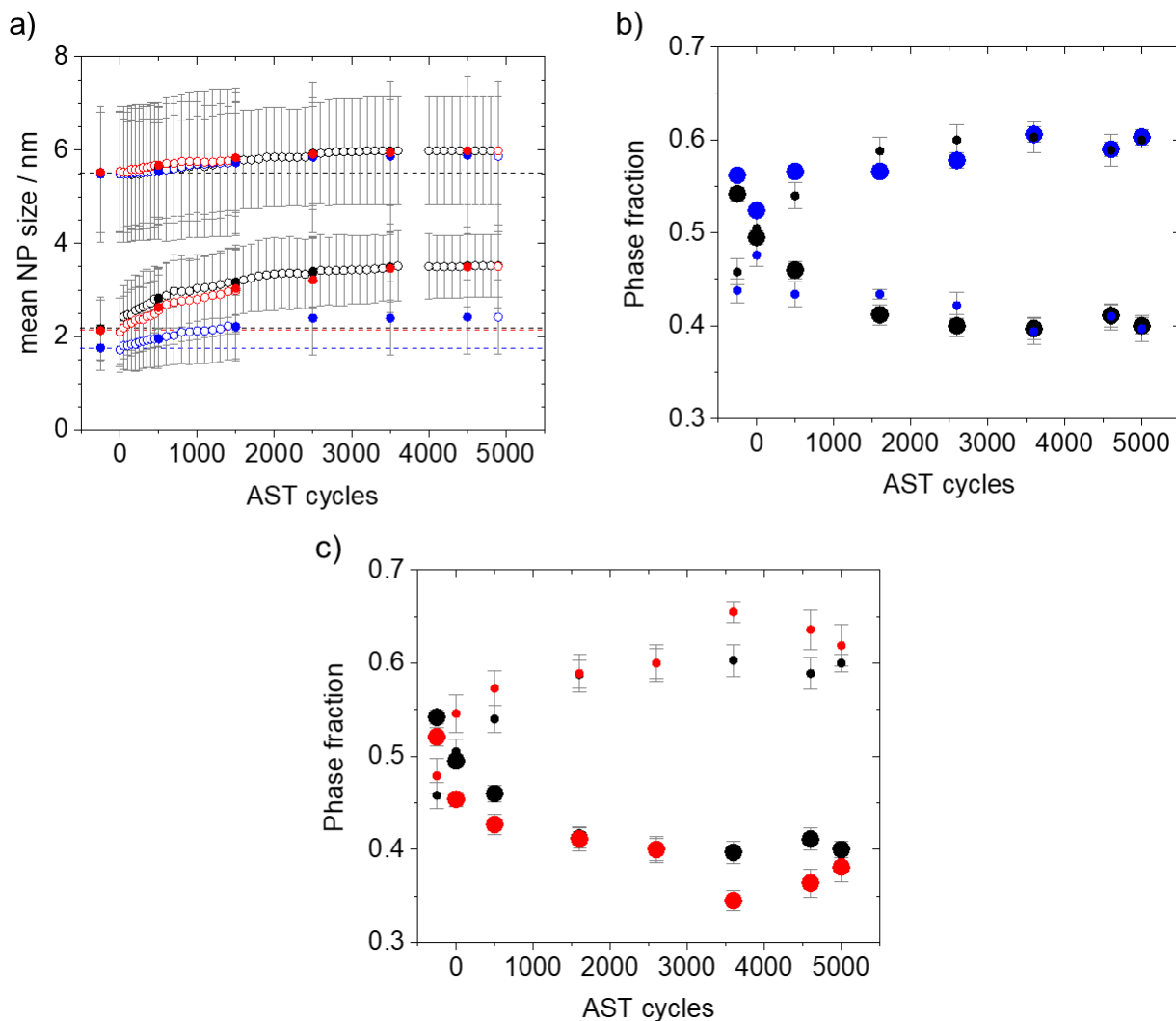
Figure 4. a) Mean particle size of the bimodal Pt NP/C catalyst plotted together with the standard deviation of a log-normal distribution applying load-cycles conditions as AST protocol in an operando cell after the AST cycles (empty circles) and after CVs (filled circles) close to the electrolyte (blue), in the middle depth (black), and deeper inside the catalyst layer. Phase fractions of the two size populations (small and large circles, for the smaller and larger size populations, respectively) obtained from Rietveld refinement of the different depth keeping the particle sizes determined via SAXS constant, b) close to the electrolyte (blue) and in the middle catalyst layer (black), c) in the middle (black) and deeper inside the catalyst layer (red) (the red filled circles are placed in front of the red circles, due to an overlap the black circles are sometimes covered). The data points of the pristine sample are given on the x-axis for a negative AST number.

4. Conclusions and future work

The results suggest that Ostwald ripening is a nanoscale phenomenon most likely triggered by Pt species mobile on the carbon support. Longer scale phenomena in an MEA are related to Pt reduction via hydrogen cross-over. A significant contribution to the degradation, however, is also related to the anchoring of the nanoparticles on the support. Both effects seem to have different dependences on the distance to the solid-liquid interface. The combination of *operando* SAXS and WAXS in grazing incidence configuration is a powerful tool that also could be used to study new degradation inhibition strategies such as the design of gradient composition and particle size distributions. Furthermore, the approach demonstrated here can be easily transferred to mechanistic studies of catalyst systems with two or more size populations consisting of different metal particles.

5. References

1.   Martens, I. *et al.* Probing the Dynamics of Platinum Surface Oxides in Fuel Cell Catalyst Layers Using in Situ X-ray Diffraction. *ACS Appl. Energy Mater.* **2**, 7772–7780 (2019).
2.   Martens, I. *et al.* X-ray transparent proton-exchange membrane fuel cell design for in situ wide and small angle scattering tomography. *J. Power Sources* **437**, 226906 (2019).

6. Publications resulting from this work
We are planning to publish the results in a joined paper. A draft has been written and corrected by all co-authors and is currently finalized.